Available online at www.sciencedirect.com
SCIENCE DIRECT®
Journal of Power Sources 118 (2003) 162–171
JOURNAL OF POWER SOURCES
www.elsevier.com/locate/jpowsour

Planar self-breathing fuel cells

A. Schmitz[a,*], M. Tranitz[a], S. Wagner[b], R. Hahn[b], C. Hebling[a]

[a]Fraunhofer Institute for Solar Energy Systems, Heidenhofstrasse 2, 79110 Freiburg, Germany
[b]Fraunhofer Institute for Reliability and Micro Integration, Gustav-Meyer-Allee 25, 13355 Berlin, Germany

Abstract

A new type of planar fuel cell based on printed circuit board (PCB) technology has been developed. This planar design consists of an open cathode side which allows a completely passive, self-breathing operation of the fuel cell. Power densities of 100 mW/cm^2 at 500 mV with hydrogen were achieved. Long-term operation for more than 1500 h has been demonstrated. The operation behavior of planar hydrogen in free-breathing PEMFC concerning stability, water management and temperature distribution are examined. The effects of diffusion layer thickness and cathode opening ratios on the performance of this fuel cell type were characterized. Moreover, the amount of water removed from the anode and the temperature distribution of the cathode side were determined.

Keywords: Planar PEMFC; Self-breathing; Open cathode; Printed circuit board (PCB)

1. Planar design of PEMFC

Portable and remotely located off-grid electronic appliances are usually powered by primary and secondary batteries. The drawbacks, especially with secondary batteries, are in many cases the insufficient energy densities. Miniaturized fuel cells potentially present beneficial opportunities for use as a supplement to or substitute for batteries [1,2]. The possibility of achieving higher energy densities with miniaturized fuel cell systems compared to conventional batteries is the driving force behind the current rapid development. State-of-the-art Li-ion batteries achieve energy densities of 350 Wh/l. The equivalent electrical energy density for hydrogen stored in metal-hydride is 1050 Wh/l and for methanol is 3000 Wh/l (1:1 molar ratio with water) [3]. To calculate the overall energy density of a fuel cell system, the volume of the fuel cell itself has to be taken into account. This implies the need to build rather small fuel cells.

For a successful integration of fuel cells into electrical appliances, the dimension of the fuel cell must be in accordance with the existing geometries of the device. The possible cavities of most devices consist of a rather flat geometry. Thus, in some cases, fuel cells with a conventional stack design might be difficult to be integrated. A flat design of fuel cells accommodates these needs—fuel cells with a planar design can, for example, be integrated in the housing of a device. As the fuel cell in this packaging concept serves as part of the housing, the volume needed for the fuel cell as power source is optimized.

The ideal planar design consists of an open cathode side to allow passive, full self-breathing operation of the fuel cell. An important advantage of the open cathode is that additional ventilation by fans is not needed. Thus, a planar fuel cell could be integrated into the back of a notebook computer or a cell phone.

2. Planar fuel cell in PCB design

The type of planar fuel cell presented in this paper is made of printed circuit boards (PCB). A standard printed circuit board consists of a fiber glass epoxy composite material (thickness 1.5 mm) and a thin copper layer (usually thickness 35 μm). In the fuel cell, the copper layer acts as a current collector. With this approach, a very small cell thickness can be achieved while maintaining a high mechanical strength.

This new approach is based on the manufacturing principles of PCB technology which is a well-known and low-cost process. Therefore, the main motivation to produce planar fuel cells in PCB technology is to achieve low costs. Quick upscaling and the ability to produce different cell types in the same process are other benefits for PCB technology. Additionally, electronic circuits can be

* Corresponding author.
E-mail address: astz@ise.fhg.de (A. Schmitz).

0378-7753/03/$ – see front matter
doi:10.1016/S0378-7753(03)00080-6

integrated on the board, which might act as electrical consumer itself or as auxiliary units with, for example, dc/dc.

In order to achieve higher voltages, a plurality of single fuel cells has to be serially connected. In a planar designed fuel cell, a serial connection is realized by electrical connection of the anode of one cell with the adjacent cathode side of the next cell. Thus, the serial connection is more challenging compared to the conventional stack design. In multilayer PCBs, several circuit layers, which are separated by insulating composite material, can overlap. Interlayer connections in the multilayer PCB technology are usually fabricated by the electroplating through holes. Thus, by using multilayer technology, the current collector layer of the anode side can be electrically connected with the current collector of the cathode side. Other options for interconnection like rivets, local welding or soldering can alternatively be used.

Additional steps which can be integrated in the process are, for example, attaching the MEA with adhesives and attaching the anode and cathode plate with adhesives. Therefore, an adapted multilayer PCB technology is ideal to realize the serial connection of a fuel cell system consisting of several single cells in a mass production process.

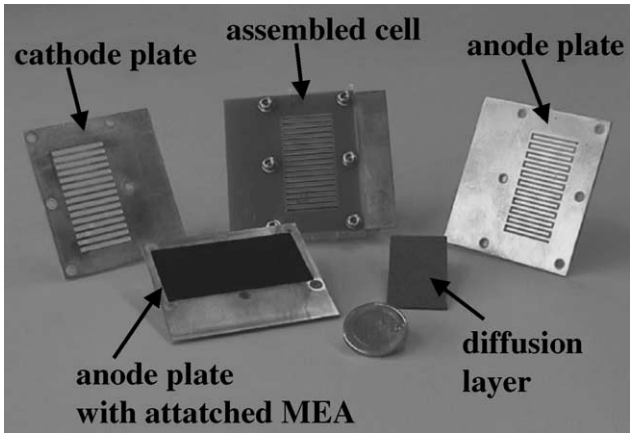

Fig. 1. Depiction of an assembled fuel cell in PCB design and components.

3. Construction of test cell and operating characteristics

The planar fuel cells used in this paper are made of ordinary printed circuit boards (Fig. 1). In the anode plate, a serpentine flow-field is machined. The cathode plate consists of parallel, rectangular openings. The electrochemical active area of this geometry has a size of 20 mm × 50 mm. The membrane electrode assembly (MEA) is attached by adhesives on the anode plate. A PRIMEA® 5510 from Gore Associates with a Pt loading of 0.3 mg/cm^2 and an ionomer thickness of 35 μm is used as MEA. Diffusion layers (Toray® carbon papers) are located between the plates and the MEA. Additionally, a thin foil with a rectangular notch in the size of the active area is sandwiched between the plates to avoid short circuits between the metal layers. This assembly is pressed together by six screws. By adjusting the torque of these screws, the contact pressure is controlled. The assembled cell has a thickness of about 3.5 mm.

Fig. 2 shows a typical polarization curve of this open, self-breathing planar PEMFC. In the maximum power point, a power density of 110 mW/cm^2 is achieved corresponding to a current density of 275 mA/cm^2 at a cell potential of 400 mV. These characteristics are in the range of power densities reported for stacks operated at room temperature [4].

As the electrical conducting elements are made of copper, corrosion in the wet environment of a PEMFC is expected. In order to avoid corrosion, the copper current collectors can be coated. The coating has to assure an impermeable cover of the copper layer to prevent any contact of the less noble

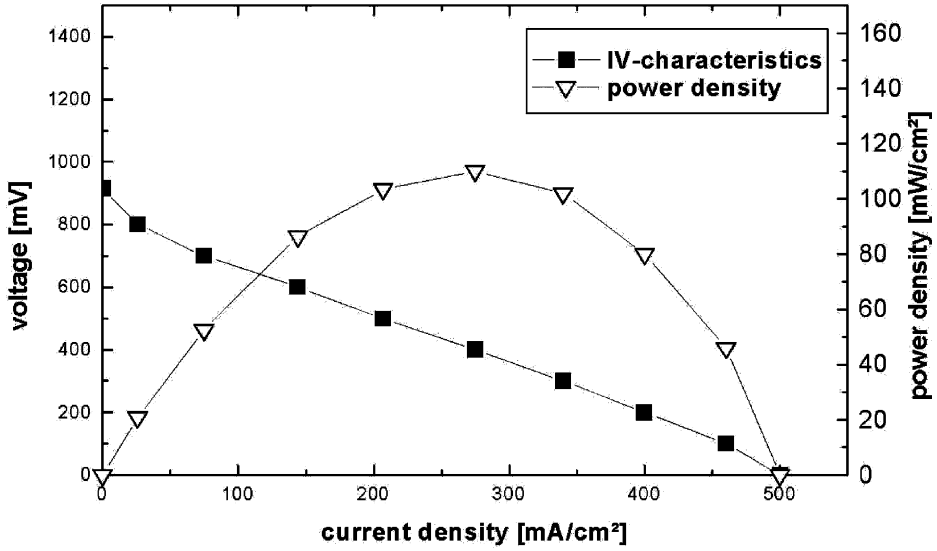

Fig. 2. Typical *I–V* and power characteristics of an open, self-breathing PEMFC in PCB design operated with hydrogen.

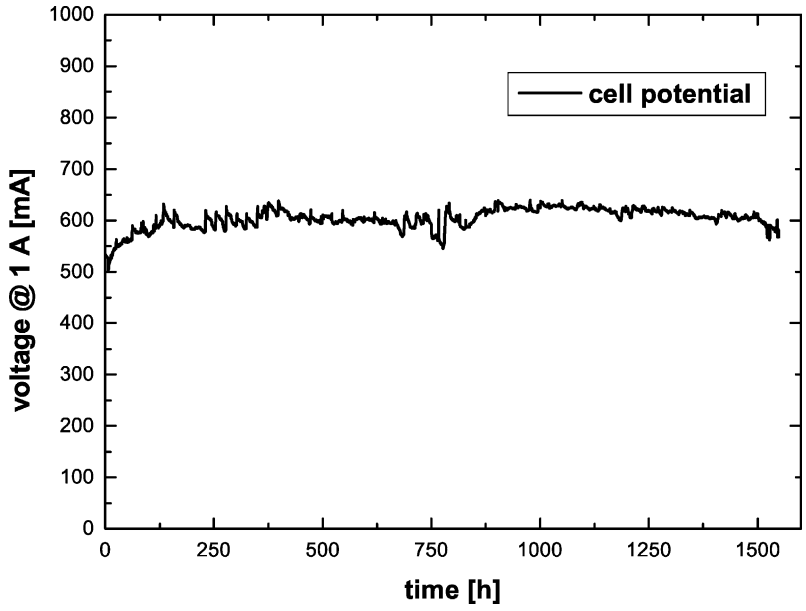

Fig. 3. Long-term performance of a PCB cell electroplated with Cr (1 μm) at a constant load of 1 A.

copper to the electrolyte and to prevent diffusion of the copper through the coating (diffusion barrier). Several coatings have been tested with corrosion measurements (potentiodynamic scans) and long-term tests [5]. The two most promising coatings for application in fuel cells have been found to be a combination of electroplated Ni (10 μm)/Au (1 μm) and an electroplated Cr (1 μm) coating.

In Fig. 3, the behavior of cell voltage under a constant load of 1 A (100 mA/cm^2) is shown for a fuel cell with a Cr coating (1 μm). Over more than 1500 h, there has no significant degradation been seen in the cell potential under load. Moreover, the fluctuations of cell potential under load are in the range of ±15% over the whole operation. This is a fairly stable result taking into account the open cathode. The operation time already achieved with the electroplated PCB cells would be adequate for the lifetime of a range of portable electronic appliances. The applied coatings are already used within the PCB industry and may be easily adapted to the serial production of planar fuel cells.

4. Influence of diffusion layer thickness

For a good performance of a fuel cell, it is necessary to achieve low contact resistance. Usually, this is realized by applying pressure between rigid and thick endplates. Thus,

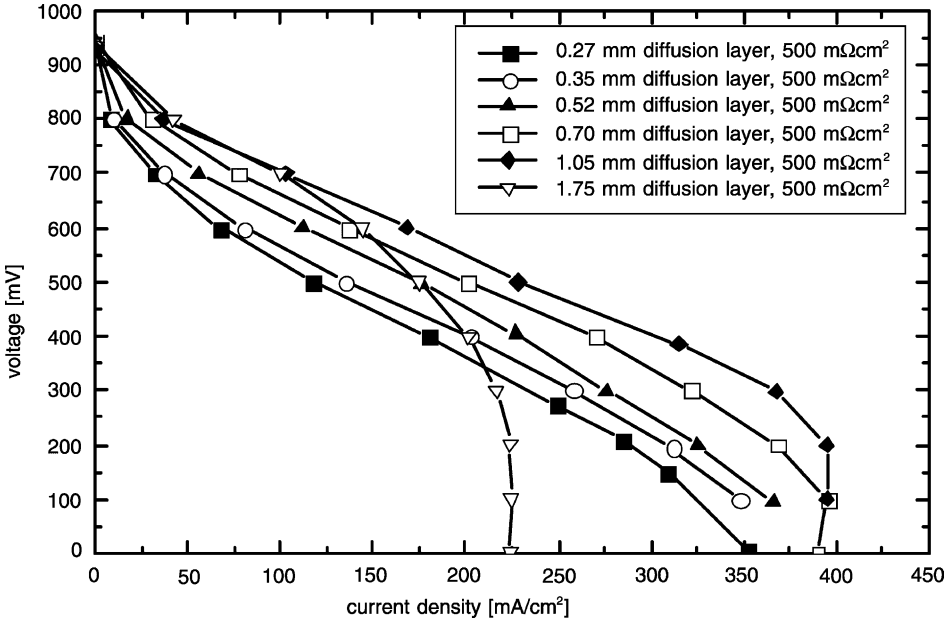

Fig. 4. Polarization curves for a variation of diffusion layer thickness.

for a planar designed cell with thin plates it is a critical issue to apply an adequate pressure. As the PCB plates consist of a composite material of fiber glass and epoxy, they offer adequate rigidness and are lightweight compared to metal plates. Nevertheless it is challenging to improve the contact resistance for a planar PCB cell.

Anode and cathode plate are not in even contact because the backing layers are sandwiched in-between. Therefore,

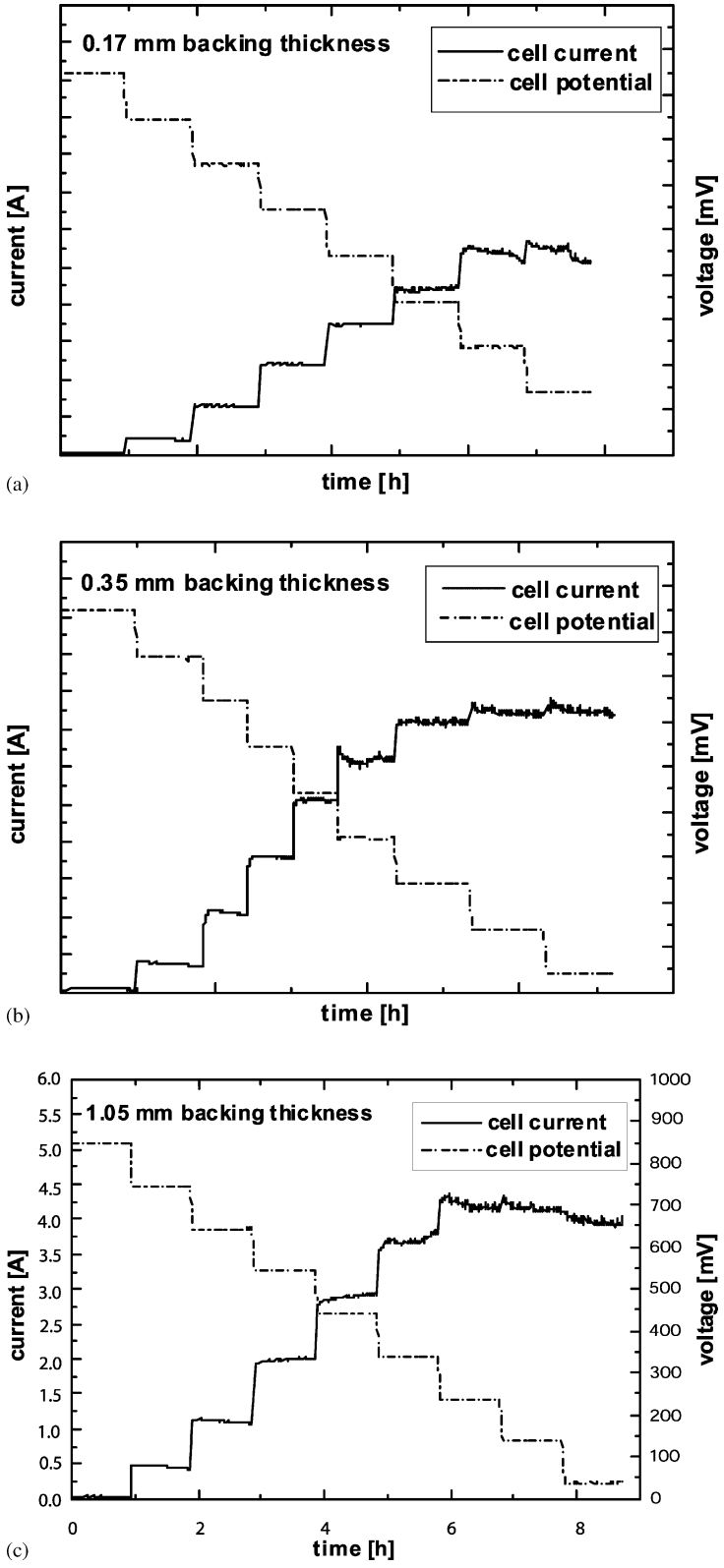

Fig. 5. *I–V* characteristics by applying potential steps for a cell with: (a) 0.17 mm thick backing; (b) 0.35 mm thick backing; (c) 1.05 mm thick backing.

the PCB plates tend to bow when the screws on the edge are tightened, potentially creating a slight gap between the backing layers and the current conducting layer in the middle of the plate. However, a thicker diffusion layer is able to compensate the gap and assures better electrical contact.

The thickness of the backing layers has been varied in order to investigate the influence on the cell performance. The backing thickness on the cathode side was increased from 0.17 to about 1.75 mm. For the thickness of 0.26 and 0.35 mm, Toray® carbon papers were used. The other thicknesses (0.52, 0.75, 1.05 and 1.75 mm) were realized by piling up combinations of the above mentioned Toray® carbon papers.

After a cell operation at a constant load of 1 A (100 mA/cm^2) over a couple of hours the cell impedance was measured. Subsequent to the resistance measurements polarization curves were recorded. The *I–V* curves and the impedance values are depicted in Fig. 4. The cell impedance was measured at a frequency of 1 kHz (HP Milliohmmeter 4388B), thereby measuring the sum of the protonic and electrical cell resistance.

In Fig. 4, it can be seen that the cell resistance drops with increasing diffusion layer thickness from 440 mΩ cm^2 for 0.26 mm thick backing layer to 170 mΩ cm^2 for a 1.75 mm thick backing layer. Because the operating conditions (constant load) assure equal water production and cell humidification the decreased cell resistance can be attributed to reduced contact resistance.

As shown in Fig. 4, a variation in diffusion layer thickness influences the cell performance. Steep declines of the *I–V* curve near short-circuit conditions imply mass transport limitations. For the thicker (1.05 and 1.75 mm) backings, mass transport limitations are seen in Fig. 4. Concerning the effects of contact resistance and mass transport limitations, a maximum in performance is achieved with diffusion layers of a thickness between 0.7 and 1.05 mm.

By measuring the potential and the current over a certain period of time, some conclusions about the stability in performance can be drawn. *I–V* characteristics were carried out by applying a constant potential for about 1 h and recording the behavior of the current. This was done in potential steps by starting at 850 mV and decreasing the potential in each step by 100 mV. Cells with backing layers of 0.17, 0.45 and 1.05 mm were characterized by this method. The results are depicted in Fig. 5a–c.

Seen at first glance, the reaction of the current for all three *I–V* characteristics is quite stable in each potential step. In most potential steps, a stable operation is reached after approximately 0.5 h.

At potentials above 650 mV, the current slightly decreases in each *I–V* characteristics. This behavior is due to a drying out effect, as the cells were supplied with unhumidified hydrogen. Below 650 mV, an increase of current behavior is seen, which is due to increased proton conductivity caused by increasing cell humidity.

Mass transfer limitations are seen at potentials of 250 mV and below, for the cell with 0.17 and 1.05 mm backing. The cell with 0.17 mm shows a decrease in cell current for potential of 250 and 150 mV. Compared to thicker backing layers, in a thin diffusion layer the water produced can block the oxygen transport more efficiently. Thus, cell flooding occurs more easily with thin diffusion layers.

5. Influence of openings

Besides the influence of the backing thickness, the size of the openings might affect the cell performance. Thus, test

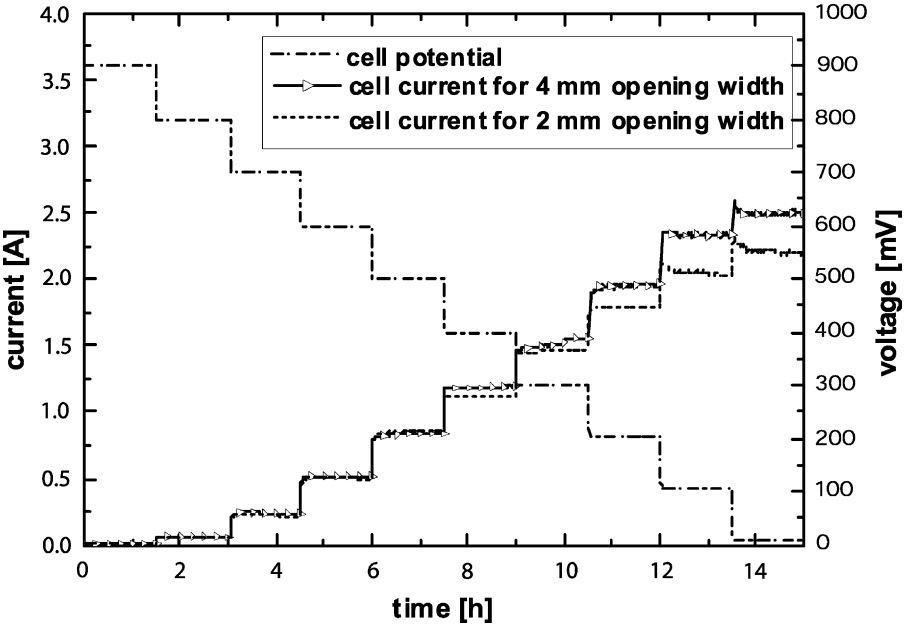

Fig. 6. *I–V* characteristics of a test cell with rectangular openings with widths of 2 and 4 mm are shown.

cells built according to the above described construction with different openings were characterized.

Cathode plates with varying opening widths were used. The cathode plates consisted of rectangular openings in the sizes of 1.5 mm × 20 mm, 2 mm × 20 mm and 4 mm × 20 mm. The width of the current collector rib between the openings was constant (1 mm). Thus, the open area ratio of the cathodes was 60, 66 and 80%, respectively. For these test cells, backings with a thickness of 0.35 mm on anode and cathode side were used. Only a slight contact pressure was applied by a torque of 0.5 N m for the screws on the edge.

Cells with two different opening ratios were characterized by the potential step method. In Fig. 6, the *I–V* characteristics of a test cell with rectangular openings with widths of 2 and 4 mm are shown. The current behavior from V_{oc} to a potential of 500 mV is nearly congruent. For lower potentials, the current for the cell with the larger openings is significantly higher.

According to the open area ratio, the contact area of the ribs to the diffusion layer is lower for the cell with the larger openings. Thus, the contact resistance of the cell with the larger openings is supposed to be higher. However, the currents are higher for the cell with the larger openings.

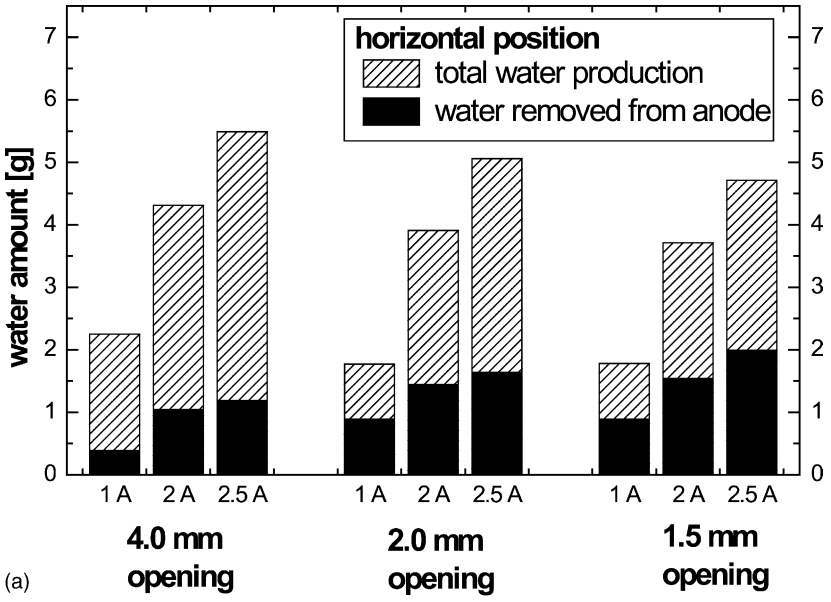

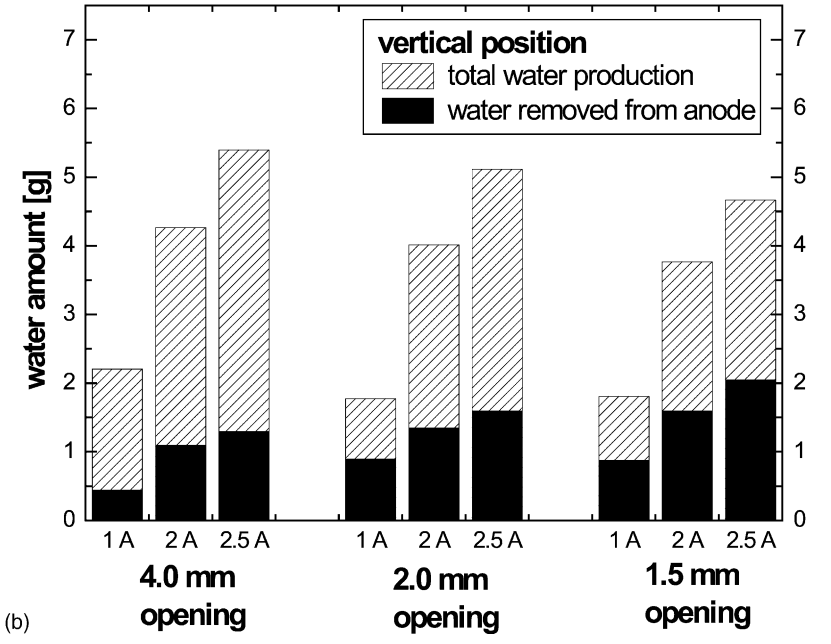

Fig. 7. Water balance for test cells with diverse cathode openings in: (a) horizontal position; (b) vertical position.

Therefore, the effects of higher contact resistances are overcompensated by improved mass transport due to larger openings.

Water is produced at the cathode of the fuel cell according to Faraday's law. Due to the open cathode, water in the gaseous phase is removed by diffusion. Moreover, water can be transported through the membrane. Water transport through the membrane can be described by back-diffusion and electro-osmotic drag [7]. Water permeates through the membrane from the cathode side to the anode side due to diffusion caused by a concentration gradient. The water transport by electro-osmotic drag is caused by proton transport from the anode side to the cathode side. The overall water transport strongly depends on the cell conditions.

The amount of water developed at the anode side can be determined by condensation of the water in the hydrogen at the cell's outlet. The hydrogen flow was passed through a glass bulb, which was plunged in cooling liquid. The liquid was cooled down to −5 °C by the use of a cryostat.

The relative humidity at the outlet of the bulb was measured by a sensor and found to be less than 10% at a temperature around 10 °C. Therefore, most of the water of the hydrogen flow condenses in the glass bulb. The accumulated water in the bulb was determined by weighing.

The determination of water removed from the anode was carried out for three cells with cathode opening widths of 1.5, 2.0 and 4.0 mm. As the orientation of the cell may have an effect on the performance, the cells were operated in two different positions: first the cells were mounted in a horizontal position with the open cathode side face up and second in a vertical position.

The cells were operated at three different constant loads of 1 A (100 mA/cm^2), 2 A (200 mA/cm^2) and 2.5 A (250 mA/cm^2). The constant load was realized with a Wenking HP88 potentiostat in galvanostatic mode. The cells were operated for a period of 8 h and subsequently, the amount of condensed water of the anode gas flow was determined. Over this period of time the total water produced in the cell at 1, 2 and 2.5 A accounts for 2.7, 5.4 and 6.7 g, respectively.

In Fig. 7a and b, the total water production and the water removed from the anode are depicted. The dependency of the anode water removal on opening size and cell current is shown in Fig. 7a for the horizontal position (open cathode upside) and in Fig. 7b for the vertical position. By comparison, no significant differences could be seen between these alternative positions. For constant cell currents with smaller opening sizes, more water is removed from the anode. Thus, with larger openings slightly more water is removed by evaporation from the open cathode.

6. Temperature distribution

Due to the exothermic reaction heat is produced in the fuel cell. The amount of heat accounts to a reversible and an irreversible part caused by overpotentials [6]. With declining cell potential the overpotential increases. Thus, increased cell temperatures are expected for decreasing cell potential.

In Fig. 8, the behavior of cell temperature for the cell with the large cathode openings (4 mm × 20 mm) at different potential steps are shown. The temperatures were measured with a Pt(1 0 0) temperature sensor, which had a rather small size of 3 mm × 5 mm. At the open cathode side, the sensor was placed in the middle of the active area at an opening with contact to the diffusion layer. The sensor on the hydrogen side was placed with contact to the back of the anode plate in the middle of the hydrogen flow-field.

As can be seen in Fig. 8, the temperature increases with declining cell potentials from room temperature to a temperature of 56 °C at the cathode side. For increasing

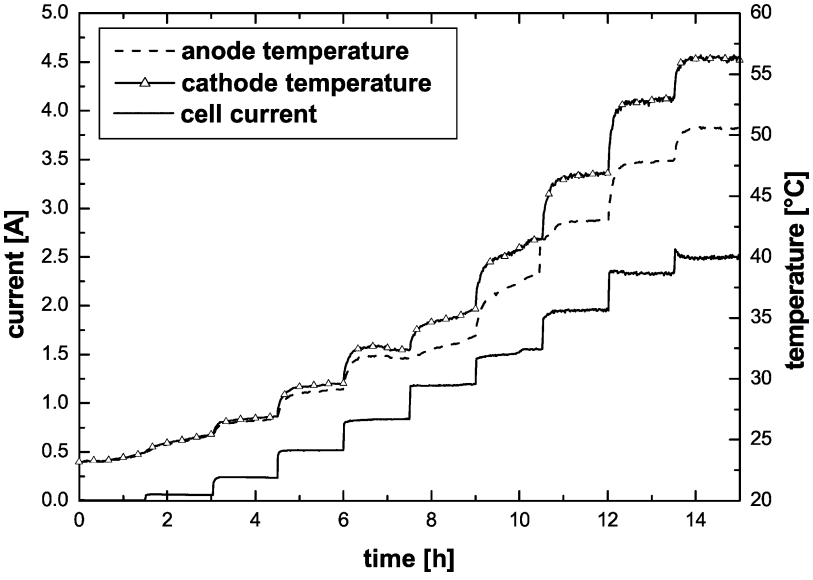

Fig. 8. Behavior of cell temperature and current for a test cell with the large cathode openings (4 mm × 20 mm).

currents, the temperature on the cathode is higher than on the anode side. For potentials from V_{oc} to a cell potential of 700 mV, nearly identically temperatures are measured. For lower potentials, the temperature difference between cathode and anode side increases.

Overpotentials on the cathode of a hydrogen fuel cell are larger than on the anode. Therefore, a larger amount of heat is produced on the cathode. Moreover, the PCB composite material has a high heat transition resistance. Therefore, the sensor on the backside of the anode flow-field measures a

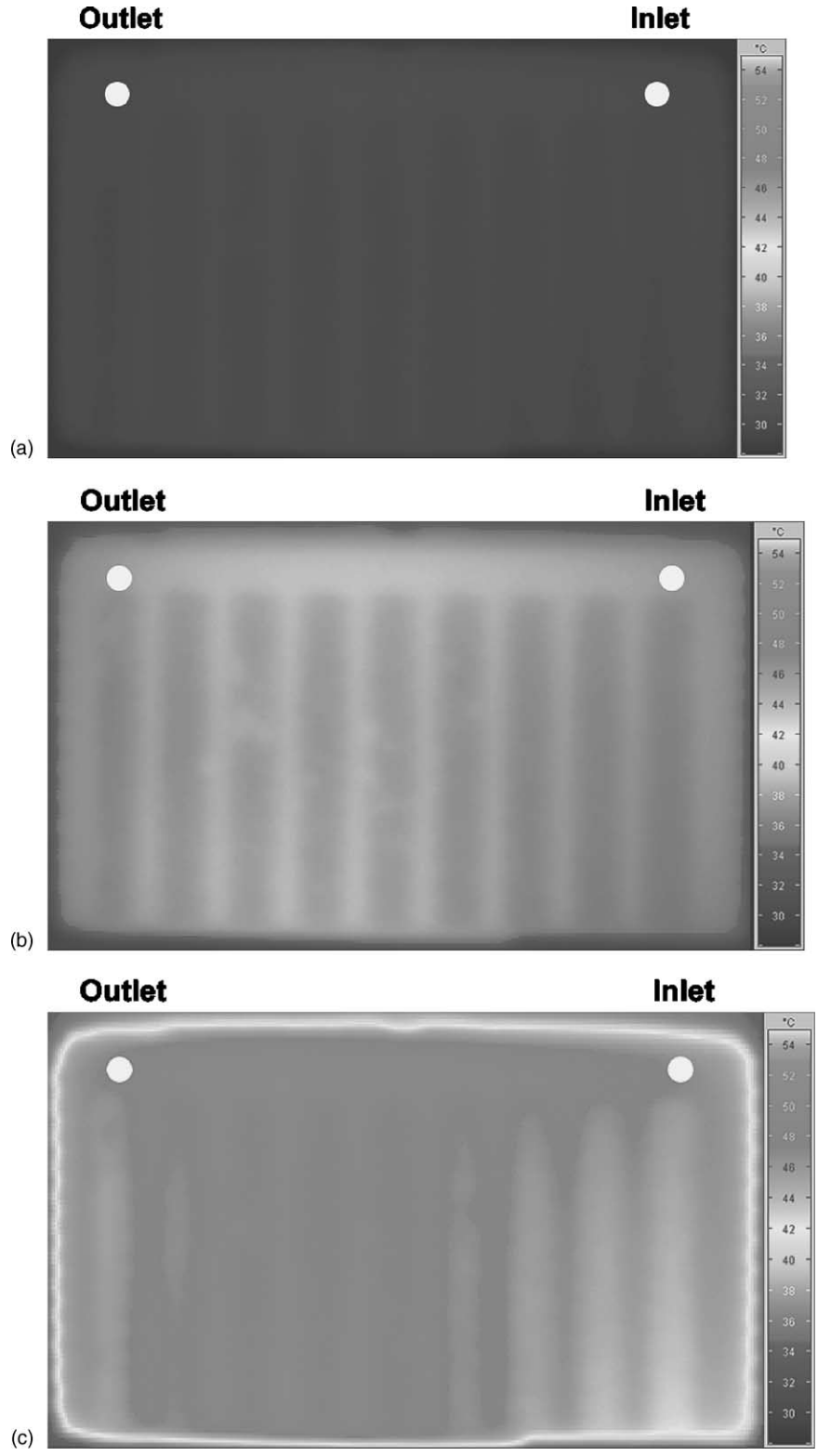

Fig. 9. Temperature distribution of the cathode side at: (a) 600 mV; (b) 400 mV; (c) 200 mV; (d) short-circuit conditions.

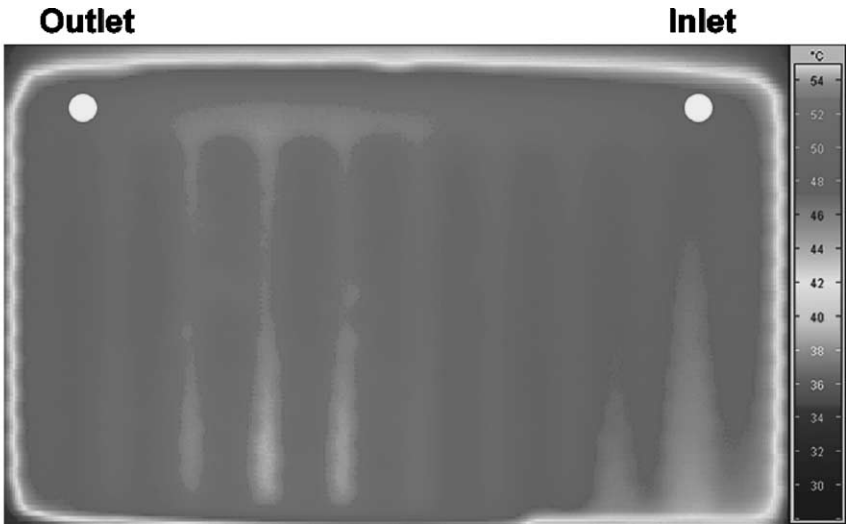

Fig. 9. (*Continued*).

slightly lower temperature than at the backing of the cathode. The maximum power point for this cell lies in the potential range of 400–500 mV. Looking at the temperatures emerged at these potentials, only a moderate warming of the cell with 35–40 °C is seen.

By the use of an infrared camera, the temperature distribution at the cathode has been measured. The utilized IR camera (Varioscan high resolution model 3021 ST from Jenoptik) is equipped with a thermal sensor, which is spectrally sensitive in the wavelength area from 8 to 12 μm.

The temperature distribution of the cathode side at four potentials (600, 400, 200 mV and short circuit) is depicted in Fig. 9a–d. The ribs (width 1 mm) and the rectangular openings (4.20 mm) can be recognized in the IR picture.

The temperature in the middle of the distributions is in good accordance with the values measured by the sensor in the middle of the cathode (Fig. 8). For exact temperature determination with the IR camera, the emissivities of the surface have to be taken into account [8].

On the IR graph, temperature differences between the temperature of the rib and the diffusion layer can be seen. These differences are due to the insulating bulk composite material and different emissivities of the diffusion layer and the PCB composite material.

At a potential of 600 mV, the temperature distribution over the whole cathode surface is rather homogenous. For potentials of 400, 200 mV and short circuit, the temperature distribution is more inhomogeneous. In these distributions, cooler areas on the left edge and the right lower corner are seen.

As the gas inlet is located on the right edge and the cells are supplied with dry hydrogen, the MEA is not as humidified as in the other parts of the cell. Therefore, the inhomogeneities on the right can be explained by decreased performance due to lower proton conductivity of the MEA.

As the composite material of the anode plate is semi-transparent, water droplets in the serpentine flow-field could be seen. Some water droplets in the left edge have evolved during cell operation at 400, 200 and 0 mV. Thus, a significantly lower temperature on the left can be explained by decreased current densities due to mass transport limitations.

7. Conclusion

Due to their flat geometry, planar fuel cells show promising perspectives for integration in housings of devices (e.g. backside of a notebook screen). The planar design offers the opportunity to design a fuel cell with an open cathode to allow fully passive, self-breathing operation. Therefore, an active air feed supplied by fans or pumps is not required.

A new type of planar fuel cell realized in printed circuit board (PCB) technology was introduced. The main motivation to manufacture fuel cells in PCB design is to achieve low costs by using a mass production process. A serial interconnection of planar arranged cells by connecting overlapping copper layers within the board can be easily realized with the multilayer technology. In addition, electronic circuits can be integrated onto the PCBs which might act as an electrical consumer itself or as an auxiliary unit.

As pure copper PCB boards would corrode in the fuel cell environment, the plates have to coated. Successfully long-term tests under a constant load with coated PCBs were demonstrated for more than 1500 h of operation without degradation.

The use of thicker diffusion layers leads to improved contact resistances. As the PCB plates of an assembled cell tend to bow in the middle, thicker diffusion layers are more able to compensate possible gaps between backing and current collector and assure an homogenous contact. Thus, the cell performance can be improved by using relative thick diffusion layers. Best results were achieved with 1.05 mm thick backing layers on the cathode. A stationary behavior for cell potentials between V_{oc} and short circuit were demonstrated by using diffusion layers thicker than 0.35 mm.

By increasing the opening ratios from 66 to 80% a significant increase in current for potentials lower than 500 mV was found. Water removed from the anode was determined by complete condensation of water in the hydrogen flow.

For several opening ratios, cell currents and cell positions, the water removed from the anode was found to be less than 30% of the total water produced. A slight decrease in removal of water from the anode was found by increasing the opening ratio from 60 to 80%.

The cell temperature in the middle of the cathode and anode side were monitored. Additionally, the temperature distribution of the cathode side was depicted by the use of an IR camera. Near short-circuit conditions, temperatures of approximately 55 °C have been measured at the cathode side. The temperature distribution at the cathode revealed inhomogeneities in the area of the gas inlet and outlet. Moderate cell temperatures (35–40 °C) have been found for maximum power point operation conditions.

References

[1] C.K. Dyer, J. Power Sources 106 (2002) 31–34.
[2] A. Heinzel et al., J. Power Sources 105 (2002) 250–255.
[3] C. Hebling, A. Heinzel, Portable fuel cell systems, Fuel Cells Bulletin (July) (2002) 8–10.
[4] M.S. Wilson, in: Proceedings of the Fuel Cell Seminar, Washington, DC, USA, 17–20 November 1996.
[5] A. Schmitz, S. Wagner, et al., Stability of planar PEMFC in printed circuit board technology, in: Proceedings of the Poster Presentation at the Ulm Eighth Electrochemical Talks, Ulm, Germany, 19–20 June 2002.
[6] J. Larminie, A. Dicks, Fuel Cell Systems, Wiley, New York, 2000.
[7] J.S. Yi, T.V. Nguyen, J. Electrochem. Soc. 145 (4) (1998) 1149–1159.
[8] J.P. Holman, Heat Transfer, McGraw-Hill, New York, 1986.